# Enhanced transient effects due to saturated absorption of recoilless $\gamma$ radiation

P. Helistö, E. Ikonen, and T. Katila
*Department of Technical Physics, Helsinki University of Technology, SF-02150 Espoo, Finland*
(Received 1 May 1986)

Prominent nonlinear transient effects due to thickness saturation are presented for the Mössbauer resonance of $^{57}$Fe. Short and intense pulses of resonant $\gamma$ radiation, resembling those obtained with synchrotron radiation, are produced using fast stepwise phase modulation. A $\gamma$-ray interferometer, based on the 0.86-Å wavelength of Mössbauer radiation, is described. Transient methods revealed the properties of a $^{57}Fe_{0.1}Rh_{0.9}$ absorber with an improvement of one order of magnitude in the statistical accuracy compared with conventional measurement techniques.

Transient techniques have been used in spectroscopic measurements since their discovery with NMR in the 1940's.[1-3] Recently, a novel type of transient was observed with optical phase switching.[4] In Mössbauer spectroscopy the first results of transient experiments were reported in 1981.[5] Most transient measurements have so far been carried out with the very narrow Mössbauer resonance of $^{67}$Zn.[5-8] In addition some $^{57}$Fe data have been published.[6,8,9] Experimentally, transient measurements are analogous to conventional and quantum beat[10,11] measurements, but because of the special nature of the transient region, some similarities with resonant pulses[12,13] of synchrotron radiation are evident.

Intensities of present Mössbauer sources are not capable of saturating the absorbers in the sense of NMR and laser spectroscopy. Yet, *thickness saturation* gives rise to highly nonlinear effects in the transmitted $\gamma$ intensity, and these are useful in transient experiments. We report here the first quantitative results from saturated transient measurements with $^{57}$Fe. The large recoilless fraction even at room temperature makes $^{57}$Fe an especially suitable Mössbauer isotope when thick absorbers are required.

A classical field model is used here to describe the interaction of source radiation with absorber nuclei. The time dependence of the radiation field transmitted through a single-line resonance absorber $E_T(t)$ can then be expressed as a sum of the original source field $E_s(t)$ and the contribution of the absorber nuclei $E_a(t)$.[8] Associated with the motion of the source $x(t)$, the phase of $E_s(t)$ is modulated by $\varphi(t)=2\pi x(t)/\lambda$, where $\lambda$ is the wavelength of the radiation. This approach appears to suffice for our case, where the intensity of the radiation traversing the absorber is detected.[14] The time dependence of the transmitted intensity $N(t)$ is given by

$$N(t)=\langle|E_T(t)|^2\rangle = N_0+2\mathrm{Re}[\langle E_s(t)E_a^*(t)\rangle]+\langle|E_a(t)|^2\rangle , \quad (1)$$

where the brackets denote averaging over the source. We point out that such a decomposition of $N(t)$ greatly facilitates the description of transient phenomena and is applicable also to other transmission Mössbauer experiments. The first (constant) term on the right-hand side is the intensity of the source at the detector, the second term describes interference between the fields due to the source and absorber, and the third term is a delayed contribution due to the absorber radiation. The saturating third term is proportional to the square of the Mössbauer thickness of the absorber $T_a$.[15] For thin absorbers it is negligible compared with the linear interference term, but when $T_a > 2$ both terms become comparable in size. The different time and phase dependences of these terms in transient experiments allow a substantial extension of the applications of Mössbauer spectroscopy.

In Fig. 1, the result of an experiment with phase switching of the 14.4-keV Mössbauer radiation of $^{57}$Fe is shown.

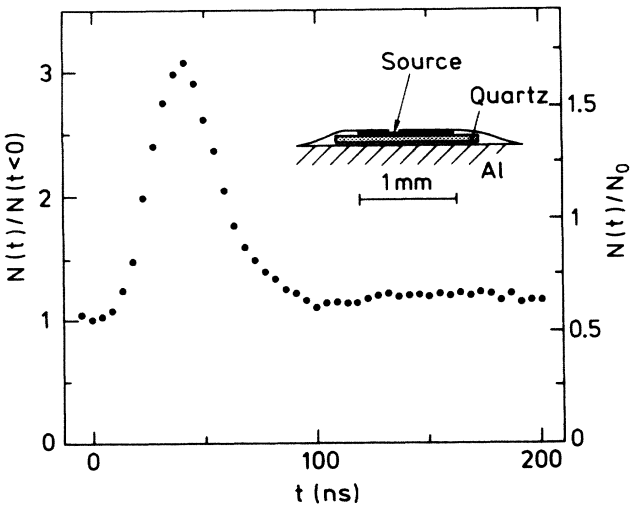


FIG. 1. Result of a phase-switching experiment when the source is rapidly displaced by approximately one $\gamma$-ray wavelength. The source, a 6-$\mu$m-thick $^{57}$Co:Rh foil with an area of 1 mm$^2$, was cemented on a x-cut quartz crystal (area $\sim$2 mm$^2$, thickness 0.08 mm). The absorber was an enriched $^{57}Fe_{0.1}Rh_{0.9}$ foil containing $\sim$0.8 mg/cm$^2$ of $^{57}$Fe. Square-wave voltage at a frequency of 200 kHz was applied across the quartz plate. The rise time of the 32-V step, starting at $t=0$, was 22 ns. The $\gamma$ quanta were collected, synchronized to the source motion, with a 0.1-mm-thick NaI(Tl) scintillator. Because of the high modulation frequency, conventional multichannel scaling units could not be used. Instead, the pulses of the scintillator were registered in a fast-slow coincidence system with the aid of a time-to-amplitude converter. The time resolution of the detector was 6 ns. Residual excitation of the mechanical resonances of the drive causes a slowly decaying component to the data.

 

Square-wave voltage is applied to a small quartz transducer to which a $^{57}$Co:Rh source[16] is attached, and the resulting change in transmission through a thick ($T_a \simeq 14$) $^{57}$FeRh absorber[16] is monitored. Before the voltage step the source and the absorber are at resonance, and $E_a \simeq e^{i\pi} E_s$ in Eq. (1). A rapid displacement of the source by $\lambda/2$ rephases $E_s$ and $E_a$, producing a sharp transmission maximum. The pulse width of 36 ns is determined by the rise time of the mechanical motion, because the voltage change in Fig. 1 causes a source displacement of approximately one wavelength. The peak-to-peak change of the transmitted intensity is more than 200% relative to the steady-state level $N(t<0)$, corresponding to 380% after correction for detector background.

As compared with the earlier results[6] obtained with $^{67}$Zn, the pulse in Fig. 1 has a much shorter duration and larger intensity. Short pulses of resonant $\gamma$ rays (full width at half maximum $\sim$22 ns) have also been produced with synchrotron radiation.[12] In contrast to synchrotron radiation, our method does not afford a high polarization and angular collimation. Nevertheless, Fig. 1 shows that short controlled $\gamma$-ray bursts can be produced with small-scale laboratory equipment. Pulse intensities of 1000–5000 $s^{-1}$ are feasible with commercial Mössbauer sources. The availability of such pulses can open new possibilities for time-resolved Mössbauer studies.

We next consider sinusoidal source motion; $x(t) = x_0 \sin(\Omega t)$, at a frequency $\Omega/2\pi$ corresponding approximately to the natural width of the resonance $\Gamma_0/2\pi$. Note that in practice the amplitude and phase of $x(t)$ do not necessarily have unique values over the source volume. In the following, variables $\chi$ and $\phi$ describe small amplitude and phase distributions around $x_0$ and $\Omega t$, and $t_r$ is the time when the source and absorber are at resonance: $dx/dt\,|_{t=t_r} = 0$, assuming zero shift between the line positions of the source and the absorber. The time evolution of the interference term, after the resonance minimum is rapidly passed, can be approximated by[8]

$$\mathrm{Re}[\langle E_s(t) E_a^*(t)\rangle] \simeq -N_0 f_s b \left\langle \left[\frac{2\pi}{\ddot{\varphi}(t_r)}\right]^{1/2} \exp[-(\Gamma_s+\Gamma_a)(t-t_r)/2] \frac{J_1(2\sqrt{b(t-t_r)})}{\sqrt{b(t-t_r)}} \times \cos\{2\pi[x(t)-x(t_r)]/\lambda - \pi/4\} \right\rangle_{\chi,\phi} . \quad (2)$$

Here $f_s$ is the recoilless fraction of the source, and $\Gamma_s$ and $\Gamma_a$ are the widths of the assumedly Lorentzian source and absorber lines, respectively. Parameter $b = T_a\Gamma_0/4$ is proportional to the Mössbauer thickness of the absorber, $J_1$ is the Bessel function of the first kind, and $\ddot{\varphi}(t_r) = d^2\varphi/dt^2\,|_{t=t_r} > (\Gamma_s+\Gamma_a+b)^2/4$. When the remaining averaging over $\chi$ and $\phi$ is performed, additional damping appears in Eq. (2).

The cosine factor of expression (2) oscillates at the instantaneous "Doppler" beat frequency between $E_s$ and $E_a$. One period of oscillation corresponds to a displacement of the source by $\lambda$, which for $^{57}$Fe is 0.860230(5) Å *in vacuo*.[17] The extremely high stability of Mössbauer resonances cannot be fully utilized in displacement measurements as counting statistics presently limit the relative accuracy to $\sim 10^{-3}$. The method of measurement is dynamical: The data are collected in the time domain and the time during which the phase coherence is preserved is determined by the lifetime of the Mössbauer state, which varies for the most common Mössbauer isotopes in the range 1 ns–10 $\mu$s (1 min for $^{109}$Ag). No separate reference beam is required to produce the interference pattern, contrary to, e.g., x-ray interferometer techniques,[18] and very small amounts of source material suffice. In Fig. 2, the result of an experiment is shown, where such a simple $\gamma$-ray interferometer is used to measure the motion produced by a quartz transducer vibrating at 1.25 MHz. The interferometric oscillations are clearly visible. According to the fit the average amplitude of the source motion is $x_0 = 3.49(1)$ Å.

Using the same assumptions as made when deriving Eq. (2), the last term of Eq. (1) becomes for $t - t_r > \sqrt{\pi/\ddot{\varphi}(t_r)}$,

$$\langle |E_a(t)|^2 \rangle \simeq N_0 f_s b^2 \left\langle \frac{2\pi}{\ddot{\varphi}(t_r)} \exp[-\Gamma_a(t-t_r)] \frac{J_1^2(2\sqrt{b(t-t_r)})}{b(t-t_r)} \times \left[1 + \frac{\sqrt{2/\pi}}{\sqrt{\ddot{\varphi}(t_r)}(t-t_r)} \sin\{2\pi[x(t)-x(t_r)]/\lambda - \pi/4\}\right] \right\rangle_{\chi,\phi} . \quad (3)$$

Since $\sqrt{\ddot{\varphi}(t_r)}$ is larger than the relaxation rates of the system, the sine term is small and the damping in Eq. (3) is mainly determined by the properties of the absorber ($\Gamma_a$ and $b$). Especially, because distributions in the modulation do not mask this decay, the result is not sensitive to experimental nonidealities. These fundamental differences between Eqs. (2) and (3) suggest an improved method for determining Mössbauer parameters.

Some results of an experimental test comparing conventional and transient methods in line-shape measurements are shown in Fig. 3. The maximum velocities of the measurements were of the same order of magnitude, but the modulation frequencies differed largely. An electromechanical velocity transducer was used to measure the spectrum in Fig. 3(a). In the measurement of Fig. 3(b) the motion was accomplished with a piezoelectric polyvinylidene fluoride (PVDF) transducer,[19] to which part of the source foil used in the conventional measurement was

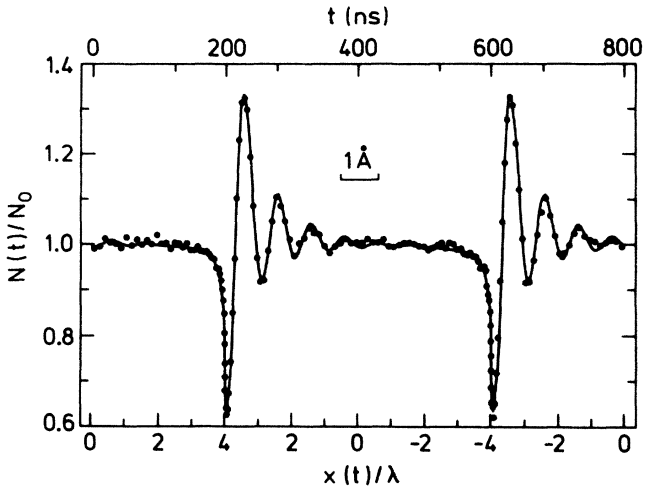


FIG. 2. Transient curve obtained with sinusoidal voltage applied to a quartz transducer (diameter 3 mm, thickness 0.15 mm). Modulation frequency was 1.25 MHz. Sources and absorbers in the measurements of Figs. 2 and 3 were as explained in Fig. 1 except for the absorber thickness of 0.4 mg/cm$^2$ of $^{57}$Fe. Separation of the adjacent zeros of the interference oscillations corresponds to a source displacement by half a wavelength (~0.43 Å). The solid curve is a theoretical fit to the data, and the displacement scale shown is linear.

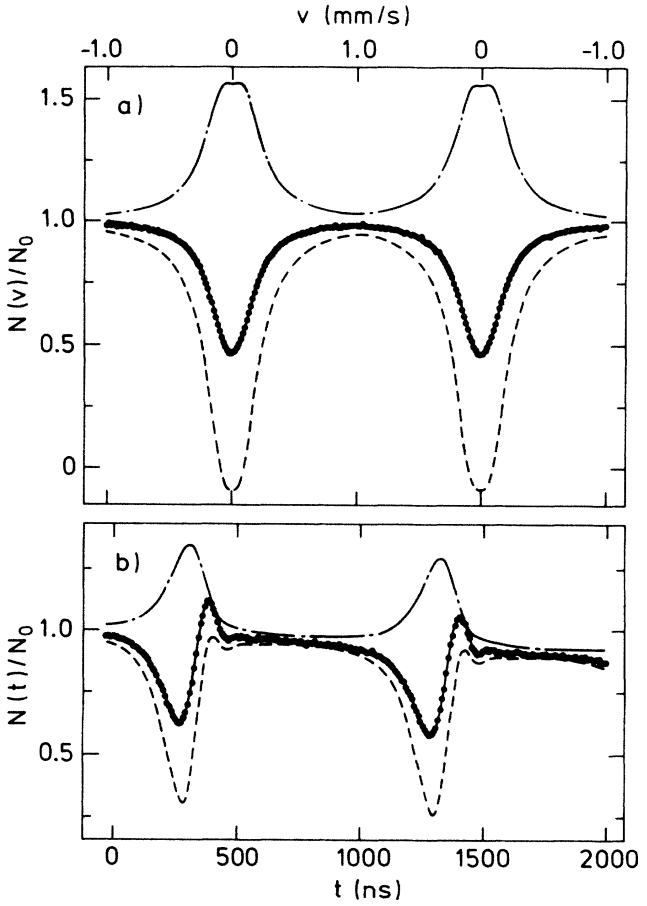


FIG. 3. (a) Unfolded result of a conventional transmission experiment with constant acceleration modulation at a frequency of 20 Hz and maximum velocity of 1.00 mm/s. (b) Transient transmission curve with sinusoidal modulation. The source was attached to a 28-$\mu$m-thick PVDF film which served as the transducer. The modulation frequency was 510 kHz and the maximum velocity 1.4 mm/s. Otherwise the setup was similar to that of Figs. 1 and 2. The contributions to the fits (solid curves) by the interference and saturating terms of Eq. (1) are shown by the dashed and dash-dotted curves, respectively.

attached. The same $^{57}Fe_{0.1}Rh_{0.9}$ absorber was used in both experiments.

In Fig. 3(a), the solid curve is a least-squares fit to the data by the transmission integral[20] applicable at low drive frequencies. Parameters $\Gamma_s$, $\Gamma_a$, and $T_a$, which determine the experimental linewidth, were varied in addition to $N_0$ and $f_s$. The fit gave statistical uncertainties as large as 40–100% for the linewidth parameters, which made the results practically unusable. The fitted curve is also shown as decomposed into the interference and saturating terms of Eq. (1). An interesting feature is the double-peaked shape of $\langle |E_a|^2 \rangle$. However, no trace of such behavior remains in the transmission integral.

The solid curve of Fig. 3(b) was obtained by fitting a general theoretical expression[8] to the data. Altogether ten parameters were variable, including $N_0$, $f_s$, $x_0$, $\Gamma_s$, $\Gamma_a$, $T_a$, and $\sigma_\phi$. Here $\sigma_\phi$ is the standard deviation of the distribution of $\phi$, assumed to have Gaussian shape.[11] Experimental nonidealities, such as source inhomogeneities and distortions of the modulation, can be treated by letting $\Gamma_s$ and $\sigma_\phi$ vary. When the fitted curve in Fig. 3(b) is decomposed in the same way as in Fig. 3(a), it is seen that the interference term shows highly damped oscillations and that the saturating term is delayed and nonoscillatory, in agreement with the approximations of Eqs. (2) and (3).

Values of $\Gamma_a$ and $T_a$ obtained from the fits of Fig. 3 and from two other transient experiments are collected in Table I. The statistical uncertainties of the results from transient measurements were 1–2 orders of magnitude smaller than those of the conventional measurement of Fig. 3(a). As the total number of counts and the signal-to-background ratio of the detector were smaller in the transient experiments, the increase in accuracy must be due to a significantly reduced correlation between the line-shape parameters. Although the values of $\Gamma_s$ and $\sigma_\phi$ displayed an experimental broadening as large as $\sim\Gamma_0$ in the source line, the results for $\Gamma_a/2\pi$ are very close to the natural linewidth $\Gamma_0/2\pi = 1.128$ MHz. The (systematic) variations in the values of $\Gamma_a$ and $T_a$ in Table I appear to be of the same order of magnitude as the statistical uncertainties. Yet, they are smaller by a factor of ~10 than the additional broadenings in the source line, reflecting the insensitivity of the transient method to experimental disturbances.

In summary, saturated transient Mössbauer spectroscopy presents several novel features for $^{57}$Fe, such as short $\gamma$ pulses, an ultrasonic $\gamma$-ray interferometer, and an improved accuracy in measurements of parameters which correlate strongly in conventional Mössbauer experiments. The results are explained by a model, which resembles semiclassical theories of NMR and laser spectroscopy.

TABLE I. Results of a conventional experiment (a) and of three transient experiments (b)–(d) with the $^{57}Fe_{0.1}Rh_{0.9}$ absorber. Values of the frequency $\Omega/2\pi$ and maximum velocity $v_0 = \Omega x_0$ of the source motion, absorber linewidth (excluding thickness broadening) $\Gamma_a/2\pi$, and Mössbauer thickness $T_a$ are given with statistical uncertainties of the fits. A fixed value of $v_0$ had to be used when fitting the conventional spectrum.

| | $\Omega/2\pi$ (kHz) | $v_0$ (mm/s) | $\Gamma_a/2\pi$ (MHz) | $T_a$ |
|---|---|---|---|---|
| (a) | 0.02 | 1.00 | $1.2 \pm 1.2$ | $7.5 \pm 3.4$ |
| (b) | 510 | $0.76 \pm 0.01$ | $1.076 \pm 0.033$ | $7.25 \pm 0.12$ |
| (c) | 510 | $1.08 \pm 0.02$ | $1.193 \pm 0.036$ | $6.69 \pm 0.14$ |
| (d) | 510 | $1.41 \pm 0.02$ | $1.257 \pm 0.048$ | $7.12 \pm 0.46$ |

Transient methods should be well adapted to studies of, e.g., relaxation and diffusion where knowledge of the actual line shape of the absorber is important. Mössbauer transients may also provide additional information when considering the interaction of light field with resonant matter, especially in the case of optically thick samples.

Discussions with Dr. K. Riski, Dr. J. Javanainen, and Dr. E. Realo are gratefully acknowledged. The authors thank Mr. J. Hietaniemi for help in the numerical data analysis and the Academy of Finland and the Emil Aaltonen Foundation for financial support.

[1]N. Bloembergen, E. M. Purcell, and R. V. Pound, Phys. Rev. **73**, 679 (1948).

[2]For a review of transient techniques in NMR, see A. Abragam, *The Principles of Nuclear Magnetism* (Oxford Univ. Press, Oxford, 1961), p. 57.

[3]Optical transient methods are treated by, e.g., R. G. Brewer, in *Frontiers in Laser Spectroscopy,* edited by R. Balian, S. Haroche, and S. Liberman (North-Holland, Amsterdam, 1977), Vol. 1, p. 342.

[4]A. Z. Genack, D. A. Weitz, R. M. Macfarlane, R. M. Shelby, and A. Schenzle, Phys. Rev. Lett. **45**, 438 (1980).

[5]P. Helistö, T. Katila, W. Potzel, and K. Riski, Phys. Lett. **85A**, 177 (1981).

[6]P. Helistö, E. Ikonen, T. Katila, and K. Riski, Phys. Rev. Lett. **49**, 1209 (1982).

[7]P. Helistö, E. Ikonen, T. Katila, W. Potzel, and K. Riski, Phys. Rev. B **30**, 2345 (1984).

[8]E. Ikonen, P. Helistö, T. Katila, and K. Riski, Phys. Rev. A **32**, 2298 (1985).

[9]E. H. Realo, K. K. Rebane, M. A. Haas, and J. J. Jõgi, Pis'ma Zh. Eksp. Teor. Fiz. **40**, 477 (1984) [JETP Lett. **40**, 1309 (1984)].

[10]G. J. Perlow, Phys. Rev. Lett. **40**, 896 (1978).

[11]J. E. Monahan and G. J. Perlow, Phys. Rev. A **20**, 1499 (1979).

[12]A. I. Chechin, N. V. Andronova, M. V. Zelepukhin, A. N. Artem'ev, and E. P. Stepanov, Pis'ma Zh. Eksp. Teor. Fiz. **37**, 531 (1983) [JETP Lett. **37**, 633 (1983)].

[13]E. Gerdau, R. Rüffer, H. Winkler, W. Tolksdorf, C. P. Klages, and J. P. Hannon, Phys. Rev. Lett. **54**, 835 (1985).

[14]J. Javanainen, P. Helistö, E. Ikonen, and T. Katila, Phys. Rev. Lett. **55**, 2063 (1985).

[15]$T_a = nf_a\sigma_0$, where $n$ is the number of resonant nuclei per unit area, $f_a$ is the recoilless fraction of the absorber, and $\sigma_0$ is the cross section of resonant absorption.

[16]Amersham Ltd., Buckinghamshire, England.

[17]*Mössbauer Effect Data Index 1976,* edited by J. G. Stevens and V. E. Stevens (Plenum, New York, 1978).

[18]R. D. Deslattes and A. Henins, Phys. Rev. Lett. **31**, 972 (1973).

[19]KYNAR Piezo Group, Pennwalt Corp., King of Prussia, PA.

[20]D. A. O'Connor, Nucl. Instrum. Methods **21**, 318 (1963).